

AP-FIM Analysis of Ultrafine Carbonitrides in Fire-Resistant Steel for Building Construction

Ryuji Uemori*
Hiroshi Tamehiro*

Rikio Chijiwa*

Abstract:

The atom-probe field-ion microscope (AP-FIM) can be used to observe materials at an atomic level and analyze their individual atoms. This report presents an application in which the AP-FIM was used to clarify the role of the combined addition of niobium and molybdenum in improving the high-temperature strength of fire-resistant steel for building construction. Findings obtained about the composition of ultrafine carbonitrides, which could not be analyzed by conventional electron microscopy, and about the elemental distribution of the carbonitride/ferrite matrix interface are briefly introduced.

1. Introduction

As part of the Ministry of Construction's comprehensive technology development project called the "Development of Comprehensive Fire-Resistant Design System for Building Fire Safety", implemented from 1982 to 1987, techniques^{*} were developed for comprehensively evaluating the fire safety of buildings from the fire and design conditions of buildings and from the performance of building materials without referring to the specifications based on the Building Standards Law. Conventional fire-resistant design methods were reviewed because of the increase in building heights and the sophistication of building design technology. This new specification nullified the old restriction that building structural steels should be covered with materials that limit their temperature to a maximum of 623 K in the event fire. It thus became possible to select fire-resistant covering methods from the combined assessment of the high-temperature strength of the steel used and the actual load of the building.

*1 Technical Development Bureau

As a result, Nippon Steel promptly developed low-yield ratio fire-resistant steels with extremely high elevated-temperature strength compared with conventional steels. Their yield strength at 873 K was guaranteed to be two-thirds of their specified room-temperature yield strength.

Research on steels with excellent high-temperature strength was carried out, centering on heat-resistant steels for medium- and high-temperature pressure vessels and boiler tubes, among other things. The heat-resistant steels are used at high temperatures for much longer periods of time than the fire-resistant steels at even higher temperatures. Earthquake resistance (low yield ratio) and other properties are also required of building structural steels. In the course of their development, building structural steels were investigated regarding the effects of alloying elements and manufacturing process conditions on the improvement of high-temperature strength and ways of lowering their yield ratio. They were also studied to establish if they are as weldable as conventional steels. As a result of these efforts, the combined addition of niobium and molybdenum was found to be extremely effective, and coupled with appropriate controlled rolling and con-

trolled cooling conditions, led to the development of fire-resistant steels with a tensile strength of 40 or 50 kgf/mm^{2,3)}.

This paper introduces the clarification by the atom-probe field-ion microscope (AP-FIM), an atomic-level analytical instrument, of the mechanism whereby the high-temperature strength of fire-resistant steels is improved by the combined addition of niobium and molybdenum, a basic fire-resistant steel strengthening principle²⁻⁴⁾. The basic principle, quantitative determination capability, and other performance details of the AP-FIM are omitted here for lack of space. For these details, see References 5) and 6).

2. Experimental Procedure

The chemical compositions of the test steels are shown in Table 1. They are the base steel, niobium (Nb) steel, molybdenum (Mo) steel, and niobium-molybdenum (Nb-Mo) steel. Each steel was melted in an electric furnace, cast into an ingot, heated at 1,523 K for 7.2 ks, rolled into a slab, reheated at 1,473K, and rolled into a plate. The rolling finish temperature was 1,223 K, and the plate thickness was 20 mm. Each plate was air cooled, aged at 873 K for 900 s, and air cooled again. Round specimens, measuring 10 mm in diameter and 40 mm in gauge length, were machined from as-rolled plates in the rolling direction and were tension tested at room and higher temperatures. High-temperature tension specimens were aged at 873 K for 900 s before they were tension tested as specified JIS G 0567.

Next, specimens for observation under the electron microscope and the AP-FIM were machined from as-rolled samples and aged samples and were used to examine their microstructures. This procedure corresponds to the microstructural comparison of fire-resistant steels at room temperature and high temperature (873 K). Using a 200-kV Hitachi Model H-800 transmission electron microscope, thin-film specimens and extraction replicas were examined. The AP-FIM was the Model FIM100 made by VG Scientific of the U.K. and had a field-ion microscope (FIM) equipped with a time-of-flight mass spectrometer.

In the AP-FIM experiment, needle-like specimens were prepared by electropolishing. Each specimen had a tip with a radius of curvature of up to 50 nm and was observed at a high magnification of several million. Individual atoms were analyzed using the field evaporation method⁶⁾ (hereinafter described as AP analysis). To examine the density distribution of precipitates, the distribution of individual precipitates and alloying elements at the precipitate/ferrite matrix interface was clarified by the ladder diagram method⁶⁾, which is used to determine the concentration distribution of atoms in the depth direction, based on their detection sequence. Prior to the electron microscope and AP-FIM experiments, specimens treated under the same conditions were observed under an optical microscope. Hardness within ferrite grains was measured concurrently. The hardness measurements

were made with a Vickers microhardness meter under a load of 0.5 kgf. The average hardness of 15 ferrite grains was taken as the hardness value for each specimen.

3. Experimental Results and Discussion

3.1 Microstructural observation by optical microscope

Photo 1 shows the optical microstructures of specimens aged at 873 K for 900 s. As evident from these observation results, the microstructure of the base steel is composed of ferrite and pearlite, with the former being predominant. The microstructures of the Nb, Mo, and Nb-Mo steels also mainly consist of ferrite. The Mo and Nb-Mo steels reveal the presence of some bainite. This is probably because their hardenability is improved by the molybdenum addition. The ferrite volume fraction is about 90 to 95% for the four steels.

3.2 Effects of microalloying elements on room-temperature strength and high-temperature strength

Fig. 1 plots the room-temperature and high-temperature yield stress (YS) of the four steels along the horizontal and vertical axes, respectively. The value of ΔYS in the figure indicates the difference in the high-temperature yield strength from the base steel. As can be seen from these results, the addition of niobium or molybdenum, or both boosts the yield strength of the Nb, Mo, and Nb-Mo steels beyond that of the base steel. The increase in

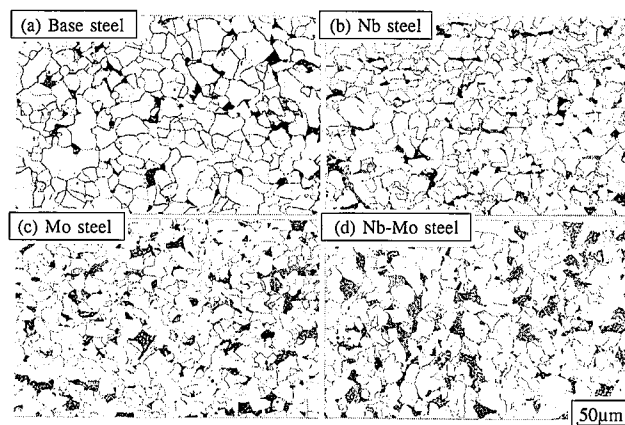


Photo 1 Optical microstructures of base steel (a), Nb steel (b), Mo steel (c), and Nb-Mo steel (d), each aged at 873 K for 900 s

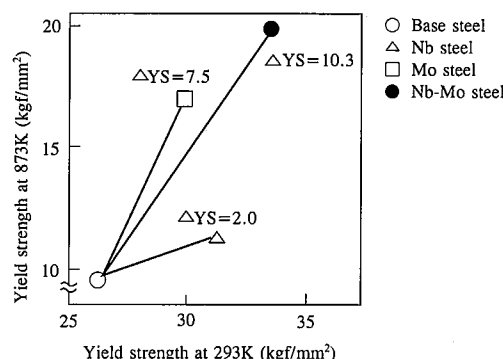


Fig. 1 Yield strength of base steel and alloy steels

Table 1 Chemical compositions of steels used (wt%)

	C	Si	Mn	Nb	Mo	Ti	Al	N
Base steel	0.099	0.23	0.91	—	—	0.016	0.015	0.0053
Nb steel	0.100	0.23	0.92	0.017	—	0.016	0.014	0.0042
Mo steel	0.112	0.25	0.93	—	0.48	0.016	0.015	0.0046
Nb-Mo steel	0.099	0.25	0.93	0.018	0.46	0.017	0.014	0.0048

the room-temperature yield strength of the Nb steel is large compared with the base steel, but the rise in the high-temperature yield strength is not as large. The high-temperature yield strength of the Mo steel is conversely greater than its room-temperature yield strength. The increase in the yield strength of the Nb-Mo steel is much greater than that of the Nb and Mo steels. A characteristic of Nb-Mo steel is that the increase in its room-temperature yield strength is equivalent to the combined rise in the high-temperature yield strength of the Nb and Mo steels, but that the increase in its high-temperature yield strength is greater than the combined rise in the high-temperature yield strength of the Nb and Mo steels. Such a remarkable rise in the high-temperature yield strength gained from the combined addition of the alloying elements niobium and molybdenum is extremely beneficial for fire-resistant steels.

Table 2 shows the room-temperature and high-temperature tensile strength (TS) of the four steels. The room-temperature and high-temperature tensile strengths of the Nb-Mo steel are both increased substantially by the combined addition of niobium and molybdenum. **Table 3** shows the ferrite grain hardness measurements of the four steels before and after aging. The preaging hardness of the alloy steels is higher than that of the base steel. The hardness increase achieved by the alloy additions agrees well with the room-temperature yield strength gain shown in **Table 2**. When the hardness change before and after aging was examined, the Mo steel was found to vary little in hardness with aging. The base steel and the Nb steel were slightly softened, and the hardness of the Nb-Mo steel was increased by aging.

3.3 Results of microstructural analysis by electron microscope and AP-FIM

3.3.1 Results of analysis by electron microscope

Given the finding that the optical microstructures of the alloy steels are predominantly composed of ferrite and according to the measured hardness values shown in **Table 3**, the strength increases resulting from the alloy additions as shown in **Fig. 1** and **Table 3** are clearly related to the ferrite hardness increases also achieved by the alloy additions. Discussion of ferrite grain obser-

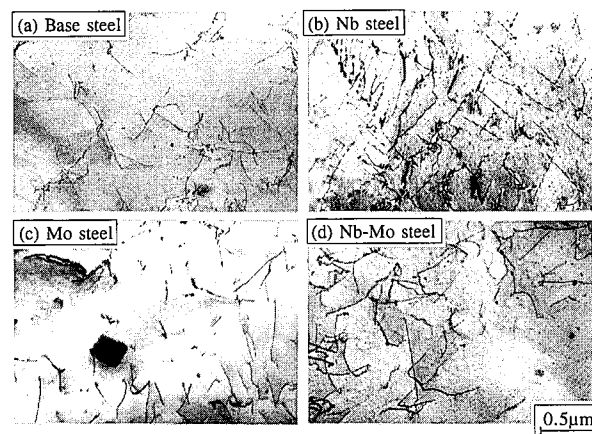


Photo 2 TEM images of specimens aged at 873 K for 900 s

vation made by electron microscope follow.

Photo 2 shows the TEM images of thin-foil specimens aged at 873 K for 900 s. The square or rectangular precipitates observed in the TEM image of the base steel in **Photo 2(a)** are those of titanium nitride (TiN), as described later. The TiN precipitates are also observed in the other steels. No other precipitates are found in the base steel.

In **Photo 2(b)**, a fine precipitate less than 20 nm in size, is visible in the Nb steel. This precipitate is not observed in the base steel and the Mo steel, so it is thought to have been derived from niobium. In the TEM image of the Mo steel in **Photo 2(c)**, needle-like molybdenum carbide (Mo_2C)⁷⁻¹⁰, known to be a major precipitate in molybdenum-bearing steels, was not found at all. In the TEM image of the Nb-Mo steel in **Photo 2(d)**, a precipitate similar to the precipitate in the Nb steel is observed. Compared with the Nb steel, extremely fine precipitates are also recognized in large amounts. Such a row-like precipitate^{6,11)} as observed during continuous cooling was also noted in the TEM image of **Photo 2(d)**. This suggests that these precipitates formed during transformation after hot rolling.

In which step the individual precipitates discussed here were formed cannot be directly determined. When these results are considered together with the results of the FIM observations presented later, it is evident that the precipitates formed during cooling and subsequent aging were added to those formed during transformation. A row-like precipitate was also confirmed in the Nb steel, but was coarser than that observed in the Nb-Mo steel. In this way, the precipitates formed in the Nb steel and the Nb-Mo steel are different in size, but extremely similar in distribution. Since this type of precipitate is not observed at all in the Mo steel, the precipitate observed in the Nb-Mo steel is presumed to be mainly composed of niobium.

According to the observation results of extraction replicas of the same steels as shown in **Photo 2**, only TiN with an average particle size of about 0.1 μm was recognized. This TiN precipitate is considered to contribute to the grain refinement of austenite. Since the four steels do not differ in TiN precipitate size and distribution, it is safe to say that the TiN precipitate is not involved in the increase in ferrite strength associated with the addition of the alloying elements niobium and molybdenum (see **Table 3**). In the Nb and Nb-Mo steels, niobium nitride (NbN) or niobium carbonitride (Nb(N,C)) is precipitated in combination with TiN, with

Table 2 Room-temperature and high-temperature tensile strength (TS)

	TS at 293K (kgf/mm ²)	TS at 873K (kgf/mm ²)
Base steel	40.0	15.0
Nb steel	42.9	16.5
Mo steel	44.5	26.7
Nb-Mo steel	48.4	28.4

Table 3 Hardness (DPN) before and after aging

	Before ageing	After ageing
	Hv	Hv
Base steel	114.0	108.0
Nb steel	127.6	121.2
Mo steel	129.5	127.3
Nb-Mo steel	141.3	144.8

TiN serving as the nuclei. These precipitates are oriented completely parallel to each other.

These results suggest that the roles played by niobium and molybdenum in increasing the hardness of ferrite, or the room-temperature and high-temperature strength of the Nb, Mo and Nb-Mo steels, are strengthening by the formation of fine precipitates for the niobium, and by solid-solution strengthening for the molybdenum. The precipitates in the Nb steel and the Nb-Mo steel cannot be identified with the electron microscope because they are too small to produce electron diffraction patterns and because the quantitative analysis of metallic elements as well as light elements cannot be performed by today's energy-dispersive spectroscopy (EDS).

3.3.2 Results of analysis by AP-FIM

The results of compositional analysis of precipitates in the Nb and Nb-Mo steels and of a study conducted to clarify the solid solution of molybdenum in the Mo and Nb-Mo steels are presented here. **Photo 3** shows the FIM images of specimens aged at 873 K for 900 s. The FIM images are sequentially described together with the results of AP analysis. The FIM images of the base steel and Mo steel in **Photo 3(a)** and **3(c)**, respectively, reveal few or no precipitates as do the TEM images of **Photo 2(a)** and **2(c)**. Needle-like Mo₃C and plate-like Mo clusters were rarely found in the aged specimen of the Mo steel. These precipitates are thus considered to have formed during aging. Since they are extremely low in frequency, however, their precipitation-strengthening action is thought to be small.

Table 4 shows the results of AP analysis of the ferrite grains performed to determine if molybdenum is dissolved in the ferrite matrix. The precipitate region was accurately separated after the FIM observation. The atomic concentration of each element was calculated from the number of the detected ions when about 5,000 ions were located by the probe hole (indicated by the arrow in **Photo 3(a)**) with its analytical region confined to the ferrite matrix.

Fig. 2 shows the depth profiles of iron and molybdenum obtained from the ferrite matrix analysis of the Nb-Mo steel (atomic concentration for every 25 ions). Even if molybdenum

Table 4 Concentrations of elements in ferrite matrix as calculated from results of AP analysis

	Atomic % of element				
	Si	Mn	Mo	Nb	Fe
Nb steel	0.46	0.80	—	0	98.74
Mo steel	0.56	0.84	0.34	—	98.26
Nb-Mo steel	0.40	0.74	0.30	0	98.56

ions are detected, the atomic concentration is 4% at most or in other words, only one out of every 25 molybdenum ions is detected at most. It can be thus concluded that the results of **Table 4** contain no information at all on the precipitates. The molybdenum concentrations in the Mo and Nb-Mo steels were found to almost agree with the molybdenum contents of the Mo and Nb-Mo steels shown in **Table 1**. It is clear that most of the molybdenum is present in solid solution as estimated from the results of observations made by electron microscopy. The results shown in **Fig. 2** also agree well with the results of the FIM observations shown in **Photo 3**.

In the Nb and Nb-Mo steels, the presence of many ultrafine precipitates was confirmed as indicated by the arrows in the FIM images of **Photo 3(b)** and **3(d)**. The particle sizes of the precipitates determined by the field evaporation method⁶⁾ are shown in **Fig. 3**. The precipitates are ultrafine, measuring 5 nm or less in average particle size. Most of the precipitates were formed in the aging step and are extremely fine compared with the precipitates (5 to 15 nm in particle size) located in the FIM images of as-rolled specimens in **Photo 4**. When the Nb and Nb-Mo steels were compared for presence or absence of molybdenum, the Nb-Mo steel is smaller in not only average particle size, but also in particle size distribution width. That is, the Mo and Nb-Mo steels contain many precipitate particles in the size range of 0 to 5 nm and do not reveal 10 nm and larger precipitate particles as recognized in the Nb steel. This result does not contradict the aforementioned electron microscopy results.

The AP analysis results of the ultrafine precipitates in the Nb and Nb-Mo steels are given in **Fig. 4**. Niobium, titanium, carbon, and nitrogen are detected in the precipitates in the Nb steel as shown in **Fig. 4(a)**. Since the detection ratio of the metallic elements niobium and titanium to the light elements carbon and nitrogen is 1:1, the ultrafine precipitates were Nb(C,N) containing minute quantities of titanium. Niobium, molybdenum, carbon,

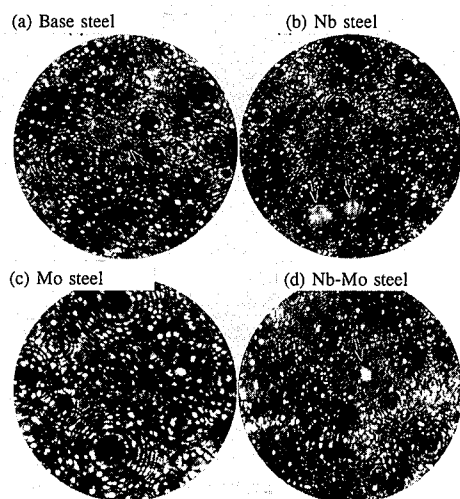


Photo 3 FIM images of specimens aged at 873 K for 900s

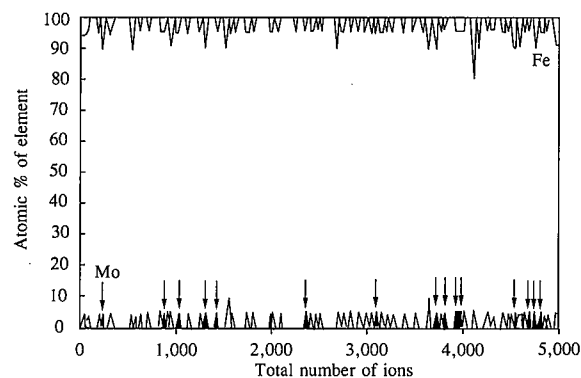


Fig. 2 Depth profiles of each element in Nb-Mo steel

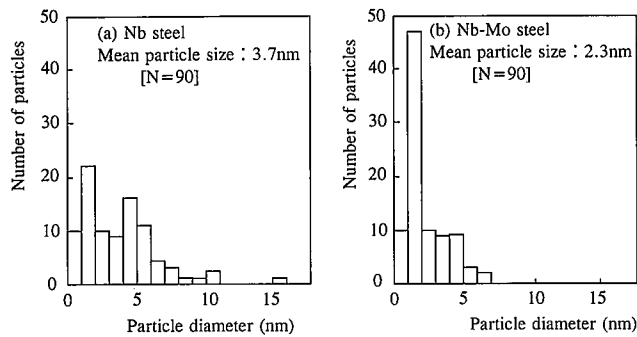


Fig. 3 Particle size distributions of precipitates measured by using field evaporation for Nb steel (a) and Nb-Mo steel (b)

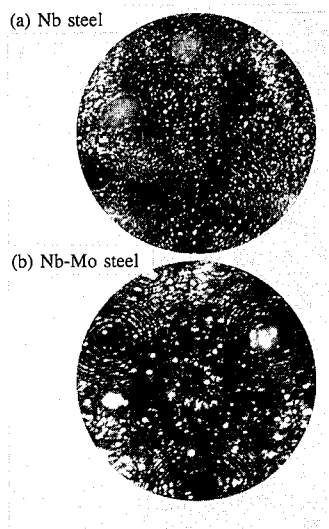


Photo 4 FIM images of as-rolled specimens

and nitrogen and were detected in the precipitates in the Nb-Mo steel as shown in Fig. 4(b). The precipitates appear to have the composition (Nb,Mo)(C,N). The number of detected ions is greater for the metallic elements than for the light elements. When the detection sequence of the elements is examined based on the ladder diagram of Fig. 5, it is evident that most of the molybdenum ions were detected at the precipitate/ferrite matrix interface. These results mean that the precipitates in the Nb-Mo steel are Nb(C,N), similar to the Nb steel, and that the molybdenum is segregated around these precipitates.

The segregation of molybdenum around the precipitates is considered to inhibit precipitate growth. For this reason, the precipitates in the Nb-Mo steel were reduced in particle size. The segregation of molybdenum was also confirmed in the as-rolled specimens before aging. The effect of aging on the molybdenum precipitates can be evaluated by the proportion of molybdenum in the metallic elements niobium and molybdenum [$\text{Mo}/(\text{Nb} + \text{Mo})$] in the precipitates. This ratio changes from 0.27 before aging to 0.42 after aging. It is obvious that aging heat treatment markedly increases the segregation of molybdenum.

The steels used in this experimental work are mainly com-

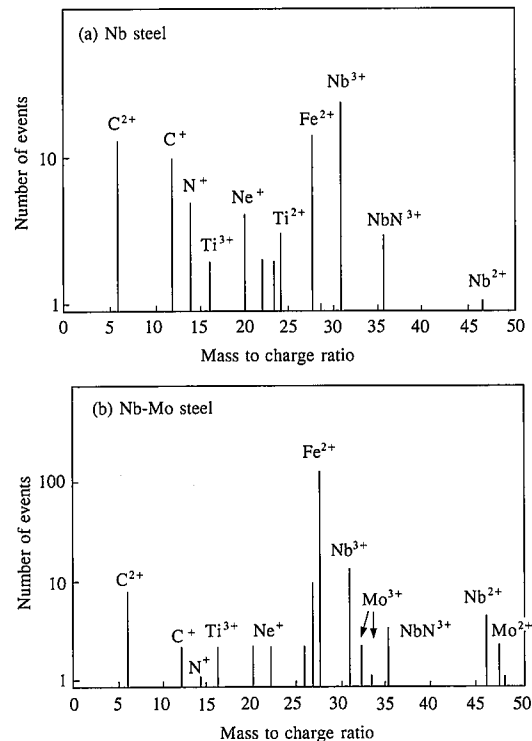


Fig. 4 AP spectra of ultrafine precipitates in Nb steel (a) and Nb-Mo steel (b)

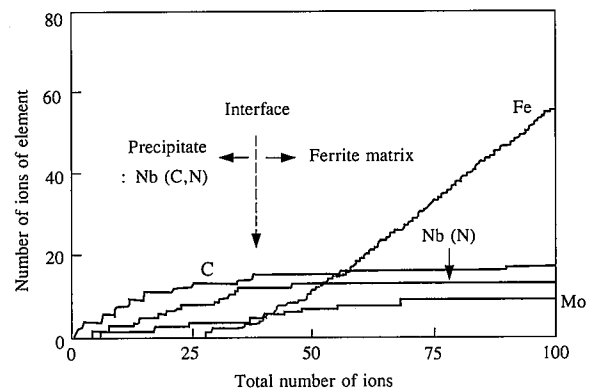


Fig. 5 Ladder diagram of fine precipitates in aged specimen of Nb-Mo steel

posed of ferrite, and the hardness of the ferrite grains themselves is increased by the addition of the alloying elements niobium and molybdenum. When these results are considered together with the results of analysis by the electron microscope and AP-FIM, there is no doubt that niobium contributes to the increase in the room-temperature and high-temperature strength of Nb-Mo steel by precipitation strengthening with NbC or Nb(C,N), and that molybdenum contributes to the increase in the room-temperature and high-temperature strength of Nb-Mo steel by solid-solution strengthening because the number of molybdenum precipitate particles is small.

The increase in the high-temperature yield strength, which is greater with the combined addition of niobium and molybdenum than with the single addition of niobium and molybdenum, can be

interpreted as the reflection of the difference in the precipitation strengthening capability of Nb(C,N) due to the presence or absence of molybdenum. Since the effect of molybdenum segregation in inhibiting the growth of Nb(C,N) can be maintained at high temperatures over a long period of time, it is beyond question that the segregation of molybdenum works to good effect in fire-resistant steels. This is supported by the fact that aging decreases the hardness of the ferrite grains in the Nb steel but increases the hardness of the ferrite grains in the Nb-Mo steel as shown in **Table 3**. It is also speculated that adding molybdenum increases the driving force (ΔG) for the precipitation of Nb(C,N) with the result that the number of precipitate particles is increased or the size of precipitate particles is reduced. The change in ΔG with the addition of 0.5% molybdenum is a mere 0.03 J/mol at most⁴⁾. The difference between the presence and absence of molybdenum is probably due to the remarkable reflection of the effect of molybdenum in inhibiting the growth of Nb(C,N).

4. Conclusions

The effect of the combined addition of niobium and molybdenum on the high-temperature strength of fire-resistant steels for building construction as investigated from a microstructural point of view has been discussed. The findings obtained may be summarized as follows:

(1)TiN (up to 0.1 μm in size) is precipitated in each of the steels used in these experiments. Especially in the Nb and Nb-Mo steels, NbN or Nb(N,C) are precipitated in combination with TiN, with TiN serving as nucleation sites. In this case, TiN and NbN are oriented completely parallel to each other.

(2)It was confirmed by the observation with the FIM that many fine precipitates are present in the ferrite matrix of the Nb and Nb-Mo steels. The AP analysis identified the fine precipitates as those of niobium carbonitride (Nb(C,N)). In the Nb-Mo steel, molybdenum was segregated at the precipitate/ferrite matrix interface. It was confirmed that the molybdenum segregation has the effect of inhibiting the growth of Nb(C,N).

(3)Most of the added molybdenum is dissolved as solute in the Mo and Nb-Mo steels. A small amount of Mo₂C and Mo-rich clusters were identified in aged specimens of Mo and Nb-Mo steels.

From the above results, it is clear that the combined addition of niobium and molybdenum increases the high-temperature strength of Nb-Mo steel through precipitation strengthening with niobium, solid-solution strengthening with molybdenum, and inhibition of the growth of Nb(C,N) with the segregation of molybdenum at high temperatures.

References

- 1) Wakamatsu, T.: Fire Safety Sic. Proc. 2nd Int. Sympo. Int. Assoc. for Fire Safety, Gaithersburg, MD, 1988, p.881
- 2) Chijiwa, R., Tamehiro, H., Yoshida, Y., Funato, K., Uemori, R., Horii, Y.: Nippon Steel Technical Report.348, 55 (1993)
- 3) Chijiwa, R., Tamehiro, H., Yoshida, Y., Funato, K., Uemori, R.: J. Jpn. Inst. Met. 32, 432 (1993)
- 4) Uemori, R., Chijiwa, R., Tamehiro, H., Morikawa, H.: Applied Surface Science. 76/77, 255 (1994)
- 5) Uemori, R., Tanino, M.: Bul. Jpn. Inst. Met. 25, 222 (1986)
- 6) Uemori, R., Saga, M., Morikawa, H.: Bul. Jpn. Inst. Met. 30, 498 (1991)
- 7) Raynor, D., Whiteman, J.A., Honeycombe, R.W.K.: J. Iron Steel Inst. 204, 349 (1966)
- 8) Dyson, D.J., Keown, S.R., Raynor, D., Whiteman, J.A.: Acta Metall. 14, 867 (1966)
- 9) Tanino, M., Nishida, T., Aoki, K.: J. Jpn. Inst. Met. 30, 894 (1966)
- 10) Uemori, R., Tanino, M.: J. Jpn. Inst. Met. 55, 141 (1991)
- 11) Ikematsu, Y., Uemori, R., Funaki, S., Morikawa, H.: Electron Microscopy. 2, EUREM 92, Granada, Spain, 1992, p.265